Effective Hamiltonian of the Jaynes-Cummings model beyond rotating-wave approximation

Yi-Fan Wang(王伊凡), Hong-Hao Yin(尹洪浩), Ming-Yue Yang(杨明月), An-Chun Ji(纪安春), and Qing Sun(孙青)
Citation: Chin. Phys. B, 2021, 30 (**6**): 064204. DOI: 10.1088/1674-1056/abd930
Journal homepage: http://cpb.iphy.ac.cn; http://iopscience.iop.org/cpb

What follows is a list of articles you may be interested in

Generation of sustained optimal entropy squeezing of a two-level atom via non-Hermitian operation

Yan-Yi Wang(王彦懿), Mao-Fa Fang(方卯发)
Chin. Phys. B, 2018, 27 (**11**): 114207. DOI: 10.1088/1674-1056/27/11/114207

Evolution of entanglement between qubits ultra-strongly coupling to a quantum oscillator

Ma Yue, Dong Kun, Tian Gui-Hua
Chin. Phys. B, 2014, 23 (**9**): 094204. DOI: 10.1088/1674-1056/23/9/094204

Entropy squeezing and atomic inversion in the *k*-photon Jaynes-Cummings model in the presence of the Stark shift and a Kerr medium： A full nonlinear approach

H R Baghshahi, M K Tavassoly, A Behjat
Chin. Phys. B, 2014, 23 (**7**): 074203. DOI: 10.1088/1674-1056/23/7/074203

Analytical approach to dynamics of transformed rotating-wave approximation with dephasing

M. Mirzaee, N. Kamani
Chin. Phys. B, 2013, 22 (**9**): 094203. DOI: 10.1088/1674-1056/22/9/094203

The population and decay evolution of a qubit under the time-convolutionless master equation

Huang Jiang, Fang Mao-Fa, Liu Xiang
Chin. Phys. B, 2012, 21 (**1**): 014205. DOI: 10.1088/1674-1056/21/1/014205

Effective Hamiltonian of the Jaynes–Cummings model beyond rotating-wave approximation*

Yi-Fan Wang(王伊凡), Hong-Hao Yin(尹洪浩), Ming-Yue Yang(杨明月), An-Chun Ji(纪安春), and Qing Sun(孙青)†

Department of Physics, Capital Normal University, Beijing 100048, *China*

(Received 17 November 2020; revised manuscript received 4 January 2021; accepted manuscript online 7 January 2021)

The Jaynes–Cummings model with or without rotating-wave approximation plays a major role to study the interaction between atom and light. We investigate the Jaynes–Cummings model beyond the rotating-wave approximation. Treating the counter-rotating terms as periodic drivings, we solve the model in the extended Floquet space. It is found that the full energy spectrum folded in the quasi-energy bands can be described by an effective Hamiltonian derived in the high-frequency regime. In contrast to the Z_2 symmetry of the original model, the effective Hamiltonian bears an enlarged $U(1)$ symmetry with a unique photon-dependent atom-light detuning and coupling strength. We further analyze the energy spectrum, eigenstate fidelity and mean photon number of the resultant polaritons, which are shown to be in accordance with the numerical simulations in the extended Floquet space up to an ultra-strong coupling regime and are not altered significantly for a finite atom-light detuning. Our results suggest that the effective model provides a good starting point to investigate the rich physics brought by counter-rotating terms in the frame of Floquet theory.

Keywords: Jaynes–Cummings model, Floquet theory, high-frequency approximation

PACS: 42.50.Pq, 42.50.–p, 37.30.+i **DOI:** 10.1088/1674-1056/abd930

1. Introduction

The Jaynes–Cummings model (JCM)[1,2] provides a fundamental paradigm to capture many important phenomena[3–13] produced by the interaction between a two-level (artificial) atom and a single-mode radiation field, e.g., the Rabi oscillations[3–7] and the entangled atom-field state.[8–10] Most of the previous works have focused in the regime of weak atom-light coupling, where the rotating-wave approximation (RWA) can be applied by neglecting the counter-rotating terms (CRTs). Nevertheless, such CRTs may become significant with the coupling strength, especially in the strong coupling regime which has been achieved in diverse systems,[14–22] and can give rise to new physics beyond RWA.[23–30] In these cases, appropriate treatment of the CRTs would be necessary.

Generally speaking, the energy spectrum of the JCM without RWA (or the Rabi model[31,32]) can be solved[33–35] with the help of numerical solutions.[36–40] However, it is not easy to analyze the physical properties of the model based on the numerical results. To gain the underlying physics in the presence of CRTs, various analytical approaches under different situations have been developed,[41–53] e.g., the generalized RWA[42] and variational methods.[44–48] Nevertheless, a general treatment of the CRTs is still desirable.

In this paper, we revisit the JCM to go beyond the RWA from a new perspective. This relies on the important observation that the CRTs can be viewed as a kind of periodical process in a transformed basis, and thus enables a general treatment within the Floquet theory,[54–59] which has been widely and successfully used to engineer nontrivial Hamiltonians in periodic driving systems recently.[60–67] Different from the previous treatments, the CRTs in the extended Floquet space would mix the neighboring Floquet modes, and give rise to unique features. We find that the full energy spectrum of the original JCM can be extracted from the numerical simulations in the extended Floquet space, and the energy spectrum is folded in each quasi-energy band due to the equivalence among different bands. In the high-frequency regime, we derive an effective Hamiltonian with an enlarged $U(1)$ symmetry, very different from the Z_2 symmetry of the original JCM. Specifically, the effects of CRTs are incorporated in a unique photon-number dependent atom-light detuning and coupling strength. Moreover, by further analyzing the energy spectrum, eigenstate fidelity and mean photon number of the resultant polaritons, we find that the high-frequency effective model can be applied up to an ultra-strong coupling regime, where the coupling strength is comparable with the frequency of the photon and is not significantly affected by finite atom-light detuning.

The paper is outlined as follows. In Section 2, we present the model and derive the high-frequency effective Hamiltonian in the Floquet theory. In Section 3, we analyze the energy spectrum, the eigenstate fidelity and the mean photon number of the polaritons of the effective model, which are compared to

*Project supported by the National Natural Science Foundation of China (Grant No. 11875195) and the Foundation of Beijing Education Committees, China (Grant Nos. CIT&TCD201804074 and KZ201810028043).

†Corresponding author. E-mail: sunqing@cnu.edu.cn

the full numerical simulations in the extended Floquet space. The influence of a finite atom-light detuning is also discussed. Finally, we give a brief summary in Section 4.

2. Model and formalism

We begin with the Jaynes–Cummings model in the presence of CRTs (or the Rabi model). In the Schrödinger picture, the total Hamiltonian of the system can be written as (we set $\hbar = 1$ throughout the paper)

$$\begin{aligned} H &= H_0 + H_{\rm int}, \\ H_0 &= \frac{\omega_{\rm a}}{2}\sigma_z + \omega_{\rm l}\hat{a}^\dagger\hat{a}, \\ H_{\rm int} &= g_0(\hat{a}+\hat{a}^\dagger)(\sigma_+ + \sigma_-). \end{aligned} \tag{1}$$

Here, $\hat{a}^\dagger$ ($\hat{a}$) creates (annihilates) a photon of the single-mode light field with frequency $\omega_{\rm l}$; σ_+, σ_- and σ_z are the Pauli matrices representing two atomic internal states with transition frequency $\omega_{\rm a}$. $H_{\rm int}$ describes the atom-light interaction with g_0 denoting the single-photon coupling strength.

To deal with the CRTs in Eq. (1), we turn to the frame rotating with frequency $\omega_{\rm l}$ by applying a unitary transformation $U(t) = {\rm e}^{{\rm i}\omega_{\rm l}(\hat{a}^\dagger\hat{a}+\frac{1}{2}\sigma_z)t}$. The Hamiltonian (1) transforms as $H \to H' = {\rm i}\frac{{\rm d}U}{{\rm d}t}U^\dagger + UHU^\dagger$, which is given by

$$\begin{aligned} H' =\ & \frac{\delta}{2}\sigma_z + g_0(\hat{a}\sigma_+ + \hat{a}^\dagger\sigma_-) \\ & + g_0(\hat{a}\sigma_-\,{\rm e}^{-2{\rm i}\omega_{\rm l}t} + \hat{a}^\dagger\sigma_+\,{\rm e}^{2{\rm i}\omega_{\rm l}t}) \end{aligned} \tag{2}$$

with $\delta = \omega_{\rm a} - \omega_{\rm l}$ being the atom-light detuning. We can realize that in this rotating frame, the CRTs exhibit time-dependent exponential factors, which just play as periodic drives with frequency $\omega \equiv 2\omega_{\rm l}$.

In the Floquet theory, the (slow) evolution in a cycle of the above periodically driven system can be described by an effective time-independent (Floquet) Hamiltonian $H^{\rm F}_{\rm eff}$. We are interested in the high-frequency regime where ω is the largest energy scale so that we can expand $H^{\rm F}_{\rm eff}$ as

$$H^{\rm F}_{\rm eff} = H^{(0)} + \frac{1}{\omega}H^{(1)} + \frac{1}{\omega^2}H^{(2)} + \mathcal{O}\left(\frac{1}{\omega^3}\right), \tag{3}$$

where

$$H^{(0)} = \frac{\delta}{2}\sigma_z + g_0(\hat{a}\sigma_+ + \hat{a}^\dagger\sigma_-) \tag{4}$$

is the time-independent part in Eq. (2) giving the well-known JCM under RWA. For the first order of $1/\omega$, we have

$$H^{(1)} = [V^{(1)}, V^{(-1)}] = \frac{g_0^2}{2}[(2\hat{n}+1)\sigma_z - I_2] \tag{5}$$

with $V^{(1)} = (V^{(-1)})^\dagger = g_0\hat{a}^\dagger\sigma_+$ and $\hat{n} = \hat{a}^\dagger\hat{a}$. I_2 is 2×2 unit matrix. One can see that $H^{(1)}$ introduces a photon-number-dependent detuning (the dynamical Stark shift) from the two-photon process. While for the second order $1/\omega^2$, we can derive (see Appendix A for detail)

$$H^{(2)} = -\frac{1}{2}\delta g_0^2[(2\hat{n}+1)\sigma_z - I_2] - g_0^3(\hat{a}\sigma_+\hat{n} + \hat{n}\hat{a}^\dagger\sigma_-). \tag{6}$$

Here the terms in the first bracket describe the contribution of a finite atom-light detuning away from resonance ($\delta = 0$). The second bracket gives a correction to the atom-light coupling with a photon-number-dependent coupling strength from the three-photon process. It is interesting to see that even though the CRTs mix subspaces with different excitation numbers $N_{\rm ex} \equiv \hat{a}^\dagger\hat{a} + \sigma_+\sigma_-$, the effective Hamiltonian conserves the total excitations, i.e., $[N_{\rm ex}, H^{\rm F}_{\rm eff}] = 0$. With this $U(1)$ symmetry, the effective Hamiltonian (3) has the same integrability with the JCM under RWA, in contrast to the Z_2 symmetry held by the original Hamiltonian (1), and thus can be solved analytically as shown in the following section.

Now, we arrive at a high-frequency effective Hamiltonian given by

$$H^{\rm F}_{\rm eff} \simeq \frac{1}{2}\tilde{\delta}_{\omega_{\rm l}}(\hat{n})\sigma_z + [g_{\omega_{\rm l}}(\hat{n})\hat{a}^\dagger\sigma_- + {\rm H.c.}] + \frac{1}{2}\delta_{\omega_{\rm l}}. \tag{7}$$

Here

$$\begin{aligned} \tilde{\delta}_{\omega_{\rm l}}(\hat{n}) &= [1 - (2\hat{n}+1)\frac{g_0^2}{4\omega_{\rm l}^2}]\delta + (2\hat{n}+1)\frac{g_0^2}{2\omega_{\rm l}}, \\ g_{\omega_{\rm l}}(\hat{n}) &= g_0(1 - \frac{g_0^2}{4\omega_{\rm l}^2}\hat{n}), \\ \delta_{\omega_{\rm l}} &= -\frac{g_0^2}{2\omega_{\rm l}} + \frac{g_0^2\delta}{4\omega_{\rm l}^2}. \end{aligned}$$

One can see that compared to the JCM with RWA, both the effective detuning $\tilde{\delta}_{\omega_{\rm l}}(\hat{n})$ and atom-light coupling $g_{\omega_{\rm l}}(\hat{n})$ are renormalized by the CRTs and depend on the photon number $\hat{n}$ as well as the light frequency $\omega_{\rm l}$.

Equation (7) is the main result and the starting point of this paper, and we will see in the following that the nontrivial contributions brought by the CRTs on the energy and mean photon number of the JCM can be well captured in the effective model with high eigenstate fidelity up to the regime with ultra-strong coupling strength.

3. Results and discussion

Before going into details of the effective model, we first discuss the typical features of the quasi-energy bands of the JCM in the extended Floquet space. As shown in Fig. 1, one can see that the quasi-energy in neighboring bands is separated by $2\omega_{\rm l}$ as expected. For $g_0/\omega_{\rm l} \ll 1$, all energy branches in different bands are well separated, where the RWA can be applied. With the increasing $g_0/\omega_{\rm l}$, the energy branches of large excitation (photon) number in neighboring bands first get touched (energy gap closing) and then those of relative smaller excitations. Until $g_0/\omega_{\rm l} \gtrsim 1$, all branches in different bands are involved. For $g_0/\omega_{\rm l} \lesssim 1$, most of the low-excitation energy branches are well isolated in each band, implying that the effect of CRTs can be included in the effective model to be shown in the following.

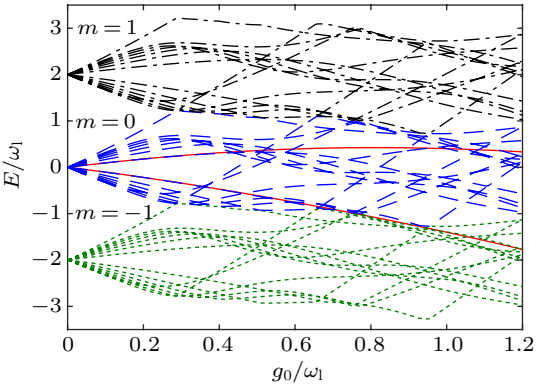

Fig. 1. The quasi-energy as a function of g_0/ω_l for $m=-1$ (green dotted), $m=0$ (blue dashed) and $m=1$ (black dash-dotted) band in the extended Floquet space for $\delta=0$. The two energy branches of the effective model for excitation number $N_{ex}=1$ are also plotted for illustration (red solid).

We now discuss the energy spectrum of the effective Hamiltonian (7). As the total excitation number N_{ex} is conserved, Eq. (7) can be solved in the subspace spanned by two product states $|g\rangle\otimes|N_{ex}\rangle$ and $|e\rangle\otimes|N_{ex}-1\rangle$ for each N_{ex}, where $|g\rangle$ ($|e\rangle$) denote the atomic ground (excited) state, and $|N_{ex}\rangle$ ($|N_{ex}-1\rangle$) is the photon Fock state with photon number N_{ex} ($N_{ex}-1$). In this basis, Hamiltonian (7) is block diagonalized with each block taking the form of

$$\begin{pmatrix} \frac{1}{2}\tilde{\delta}_{\omega_l}(N_{ex}-1)+\frac{1}{2}\delta_{\omega_l} & \sqrt{N_{ex}}g_{\omega_l}(N_{ex}) \\ \sqrt{N_{ex}}g_{\omega_l}(N_{ex}) & -\frac{1}{2}\tilde{\delta}_{\omega_l}(N_{ex})+\frac{1}{2}\delta_{\omega_l} \end{pmatrix}, \quad (N_{ex}>0).$$

After a straightforward diagonalization, we can obtain two energy branches of the polariton for each N_{ex},

$$E_{\pm}^{(N_{ex})} = \delta_{\omega_l} \pm \sqrt{\left(\frac{\delta}{2}-N_{ex}\delta_{\omega_l}\right)^2 + N_{ex}[g_{\omega_l}(N_{ex})]^2}, \quad (N_{ex}>0). \tag{8}$$

Notice that $N_{ex}=0$ gives the ground state with energy $E_g=-\delta/2+\delta_{\omega_l}$.

In Fig. 2, we plot the lower energy branch E_- as a function of coupling strength g_0 at resonance $\delta=0$ for the interested low excitation numbers N_{ex}. For comparison, we have also presented the results from RWA and a full numerical simulation beyond high-frequency approximation (HFA) in the extended Floquet space (see Appendix B for detail). We can see that the RWA is mainly justified for $g_0/\omega_l \ll 1$, and the deviations from the numerical results become remarkable with the increasing atom-light coupling strength g_0, indicating the breakdown of RWA in a strong coupling regime. On the other hand, the effective Hamiltonian gives a quite good approximation for $g_0/\omega_l \lesssim 0.6$ and works qualitatively well up to $g_0/\omega_l \approx 1$. The validity of the HFA in this regime resides in the well separation of quasi-energy bands for not too large g_0. While for $g_0/\omega_l \gg 1$, the different Floquet bands get involved and the HFA is no longer applicable.

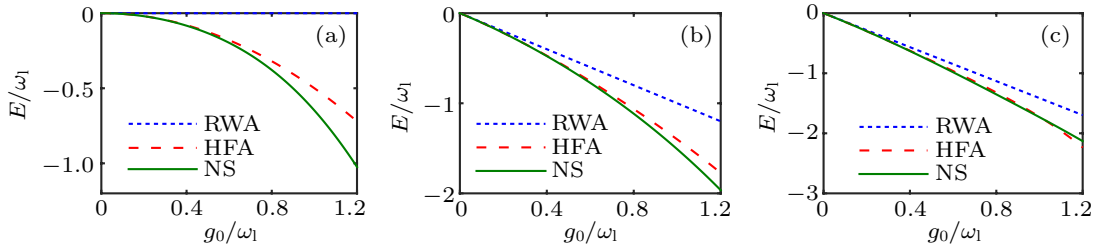

Fig. 2. The lower-branch energy E_-/ω_l as a function of g_0/ω_l of the HFA (red dashed) for excitation number $N_{ex}=0$ (a), 1 (b), and 2 (c) at resonance $\delta=0$. The corresponding energy branches under RWA (blue dotted) and by numerical simulations (NS, green solid) are also plotted for comparison.

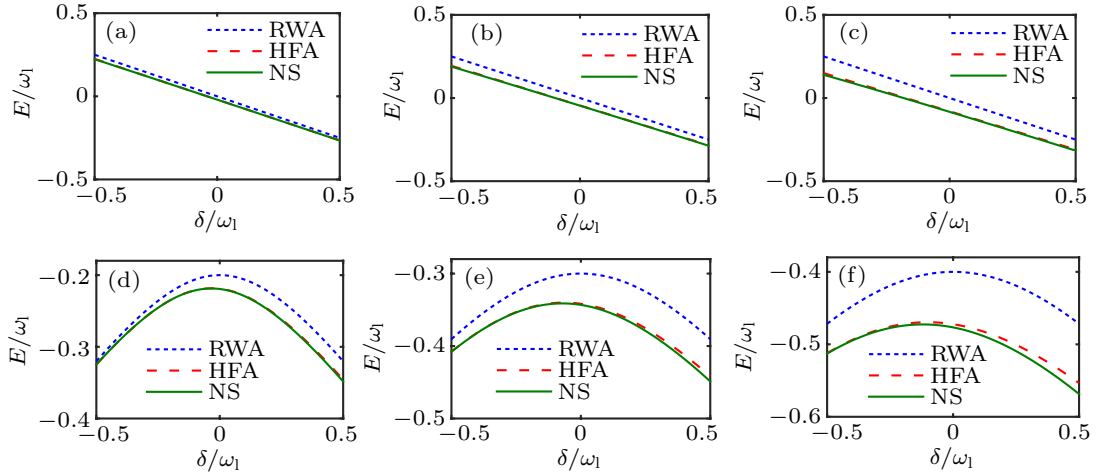

Fig. 3. The lower-branch energy E_-/ω_l as a function of atom-light detuning δ/ω_l under RWA (blue dotted), HFA (red dashed) and NS (green solid) for coupling strength $g_0/\omega_l=0.2$ [(a), (d)], 0.3 [(b), (e)], and 0.4 [(c), (f)]. Here, the excitation number is $N_{ex}=0$ for (a)–(c) and $N_{ex}=1$ for (d)–(f), respectively.

We further investigate the effect of finite atom-light detuning. We first notice that even for a bare resonance $\delta = 0$, the effective detuning in the high-frequency model may become finite with $N_{\rm ex} g_0^2/\omega_{\rm l}$. This can signal the departure of the RWA due to the CRTs. Figure 3 shows the lower branch of energy E_- as a function of atom-light detuning δ for fixed coupling strength and excitation number. It is readily to see that the HFA works quite well in a considerable parameter regime from negative to positive detuning. Moreover, the spectrum is generally asymmetric with respect to the detuning δ, in contrast to the symmetric spectrum of the RWA for $N_{\rm ex} \geq 1$. As the resonance point is shifted to $\delta = \frac{2N_{\rm ex} g_0^2 \omega_{\rm l}}{N_{\rm ex} g_0^2 - 2\omega_{\rm l}^2} < 0$ in the effective model, the deviation from the numerical results is relative large for positive detuning (see Fig. 3(f) for a reference).

The agreement of the energy spectrum between the effective model and the full numerical simulations becomes more transparent when we examine the fidelity of the eigenstate. To this end, we write the eigenstate of the lower branch in the photon-dressed basis as

$$|\psi\rangle^-_{N_{\rm ex}} = C|e\rangle|N_{\rm ex}-1\rangle + D|g\rangle|N_{\rm ex}\rangle \tag{9}$$

with

$$|C|^2 = \frac{1}{2} - \frac{(\delta - 2N_{\rm ex}\delta_{\omega_{\rm l}})\sqrt{(\delta - 2N_{\rm ex}\delta_{\omega_{\rm l}})^2 + 4N_{\rm ex}[g_{\omega_{\rm l}}(N_{\rm ex})]^2}}{2(\delta - 2N_{\rm ex}\delta_{\omega_{\rm l}})^2 + 8N_{\rm ex}[g_{\omega_{\rm l}}(N_{\rm ex})]^2}, \tag{10}$$

$$|D|^2 = \frac{1}{2} + \frac{(\delta - 2N_{\rm ex}\delta_{\omega_{\rm l}})\sqrt{(\delta - 2N_{\rm ex}\delta_{\omega_{\rm l}})^2 + 4N_{\rm ex}[g_{\omega_{\rm l}}(N_{\rm ex})]^2}}{2(\delta - 2N_{\rm ex}\delta_{\omega_{\rm l}})^2 + 8N_{\rm ex}[g_{\omega_{\rm l}}(N_{\rm ex})]^2}. \tag{11}$$

Here C and D are the complex amplitudes in the dressed excited and ground state respectively satisfying $|C|^2 + |D|^2 = 1$. We introduce the time-averaged fidelity $\bar{F}$ in a cycle between the eigenstate of the effective model $|\psi\rangle_{N_{\rm ex}}$ and the Floquet eigenstate $|\psi(t)\rangle$ (see Appendix B), which is defined by

$$\bar{F} \equiv \frac{1}{T}\int_0^T \langle\psi(t)|\psi\rangle_{N_{\rm ex}} {\rm d}t. \tag{12}$$

In Fig. 4, we give the fidelity distribution in the g_0–δ plane for the lower branch of $N_{\rm ex} = 1$. We find $\bar{F} \geq 0.9$ in a broad parameter regime, suggesting that the effective model is a quite good approximation of the JCM.

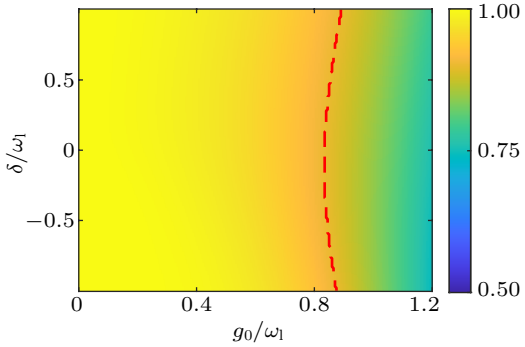

Fig. 4. The time-averaged fidelity $\bar{F}$ between the eigenstate of the effective model and the Floquet eigen-mode in the g_0–δ plane for the lower branch with $N_{\rm ex} = 1$. The red dashed line labels $\bar{F} = 0.9$.

So far, we have discussed the polariton energy spectrum and the eigenstate fidelity of the effective model. It is also worthy to obtain the mean photon number of the polariton, which can be measured in experiment. Taking use of the explicit form of the eigenstate, the mean photon number of the lower branch is given by

$$n_{\rm ph} \equiv \langle\hat{a}^\dagger\hat{a}\rangle = |C|^2(N_{\rm ex}-1) + |D|^2 N_{\rm ex}. \tag{13}$$

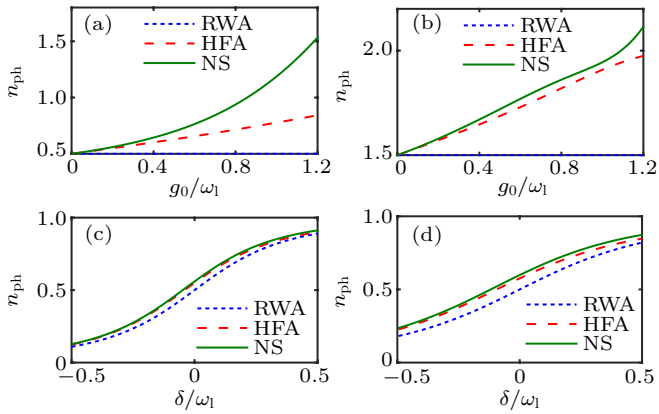

Fig. 5. The mean photon number $n_{\rm ph}$ of the lower branch as functions of $g_0/\omega_{\rm l}$ [(a), (b)] and $\delta/\omega_{\rm l}$ [(c), (d)] under RWA (blue dotted), HFA (red dashed) and NS (green solid). Other parameters are: [(a), (b)] $\delta = 0$, $N_{\rm ex} = 1$ and 2; [(c), (d)] $N_{\rm ex} = 1$, $g_0/\omega_{\rm l} = 0.2$ and 0.3.

In Figs. 5(a) and 5(b), we plot the mean photon number $n_{\rm ph}$ as a function of coupling strength g_0 at resonance for the lower branch of excitation number $N_{\rm ex} = 1$ and 2. Different from the RWA which gives a coupling-independent constant value, the mean photon number in the lower branch of the effective model increases with the coupling strength, in accordance with the numerical results, due to the fact that the contributions from states with higher excitation numbers brought by CRTs become significant, which are incorporated in the photon-dependent coupling strength and detuning in the effective Hamiltonian (7). Figures 5(c) and 5(d) show the dependence of mean photon number $n_{\rm ph}$ on the detuning δ. Similar to the energy discussed above, the mean photon number predicted by the effective model agrees quite well with the numerical simulation even for large detuning $|\delta| \gg 0$. Specific for $\delta \ll 0$, the component $\sim|e\rangle \otimes |N_{\rm ex}-1\rangle$ in the wave function is

dominated and $n_{\rm ph} \to 0$. While for $\delta \gg 0$, the atom is mainly in the ground state with a nearly free photon, $|g\rangle \otimes |N_{\rm ex}\rangle$, giving rise to $n_{\rm ph} \to 1$.

4. Conclusion

We have studied the JCM in the frame of Floquet theory. By treating the CRTs as periodic drives, we solve the model in the extended Floquet space and derive an effective Hamiltonian with enlarged $U(1)$ symmetry in the regime of high "driving" frequency. We find that the energy spectrum as well as the mean photon number predicted by the effective model agrees well with the numerical simulations of high eigenstate fidelity in a broad parameter regime even for an ultra-strong atom-light coupling, where the coupling strength is comparable with the photon frequency and the RWA generally breaks down. The Floquet method developed in this work provides a systematic and efficient way to study the nontrivial physics brought by CRTs, and can also be applied to other situations, e.g., the multimode atom-cavity systems, coupled atom-cavity arrays and dispersive atom-light couplings.

Appendix A: Derivation of the effective Hamiltonian

In this paper, the rotational Hamiltonian (2) can be written as

$$H' = H^{(0)} + V^{(1)}\,\mathrm{e}^{\mathrm{i}\omega t} + V^{(-1)}\,\mathrm{e}^{-\mathrm{i}\omega t}, \tag{A1}$$

where $H^{(0)} = g_0(\hat{a}\sigma_+ + \hat{a}^\dagger\sigma_-) + \delta\frac{\sigma_z}{2}$, $\omega = 2\omega_{\rm l}$, $V^{(1)} = g_0\hat{a}^\dagger\sigma_+$, $V^{(-1)} = g_0\hat{a}\sigma_-$.

According to the Floquet theory,[54] the long-time evolution of the above periodic Hamiltonian can be described by an effective time-independent Floquet Hamiltonian $H^{\rm F}_{\rm eff} = \sum_{n=0}^{\infty}\frac{1}{\omega^n}H^{(n)}$ in an expansion of $1/\omega$. When ω is the largest energy scale, we can apply the high-frequency approximation by keeping the expansion series to the second order,[55]

$$H^{\rm F}_{\rm eff} \approx H^{(0)} + \frac{1}{\omega}H^{(1)} + \frac{1}{\omega^2}H^{(2)} \tag{A2}$$

with $H^{(1)} = \frac{g_0^2}{2}[(2\hat{n}+1)\sigma_z - I_2]$ given in the main text, and

$$H^{(2)} = \frac{1}{2}([[V^{(1)},H^{(0)}],V^{(-1)}] + [[V^{(-1)},H^{(0)}],V^{(1)}]). \tag{A3}$$

A straightforward calculation gives

$$\begin{aligned}&[[V^{(1)},H^{(0)}],V^{(-1)}]\\ &= [g_0^2\hat{a}^\dagger\hat{a}^\dagger\sigma_z - g_0\delta\hat{a}^\dagger\sigma_+, V^{(-1)}]\\ &= -2g_0^3\hat{n}\hat{a}^\dagger\sigma_- - \frac{g_0^2\delta}{2}[(2\hat{n}+1)\sigma_z - I_2],\end{aligned} \tag{A4}$$

and $[[V^{(-1)},H^{(0)}],V^{(1)}] = [[V^{(1)},H^{(0)}],V^{(-1)}]^+ = -2g_0^3(\hat{n}+1)\hat{a}\sigma_+ - \frac{g_0^2\delta}{2}[(2\hat{n}+1)\sigma_z - I_2]$. To sum up, we arrive at the final form of the second term given in the main text.

Appendix B: Numerical simulation in the extended Floquet space

B1. The matrix of the quasi-energy operator

In the extended Floquet space, the basis states for the Hamiltonian H' can be written as $|\alpha m(t)\rangle = \{|e,n\rangle\,\mathrm{e}^{\mathrm{i}m\omega t}, |g,n\rangle\,\mathrm{e}^{\mathrm{i}m\omega t}\}$, where $n \in \mathbb{N}$ is the photon number and $m \in \mathbb{Z}$ is the 'photon' index. The time-periodic-averaged matrix of the quasi-energy operator $G = H' - \mathrm{i}\mathrm{d}_t$ can be written as[56]

$$\begin{aligned}&\frac{1}{T}\int_0^T \langle\alpha' m'(t)|G|\alpha m(t)\rangle\,\mathrm{d}t\\ &= \langle\alpha'|H'_{m'-m}|\alpha\rangle + \delta_{m'm}\delta_{\alpha'\alpha}m\omega\\ &= \begin{pmatrix} \ddots & \vdots & \vdots & \vdots & \vdots & \ddots\\ \cdots & H'_0-\omega & H'_{-1} & 0 & 0 & \cdots\\ \cdots & H'_1 & H'_0 & H'_{-1} & 0 & \cdots\\ \cdots & 0 & H'_1 & H'_0+\omega & H'_{-1} & \cdots\\ \cdots & 0 & 0 & H'_1 & H'_0+2\omega & \cdots\\ \ddots & \vdots & \vdots & \vdots & \vdots & \ddots \end{pmatrix},\end{aligned} \tag{B1}$$

where $H'_{m'-m} = \frac{1}{T}\int_0^T H'\,\mathrm{e}^{\mathrm{i}(m-m')\omega t}\mathrm{d}t$ is a matrix as the Fourier transformation of the Hamiltonian H' and has the form

$$H'_{m'-m} = \begin{cases} g_0(\hat{a}\sigma_+ + \hat{a}^\dagger\sigma_-) + \delta\frac{\sigma_z}{2}, & m'=m;\\ g_0\hat{a}\sigma_-, & m'-m=-1;\\ g_0\hat{a}^\dagger\sigma_+, & m'-m=1. \end{cases} \tag{B2}$$

As the parity of the excitation number in the Hamiltonian H' is conserved (even or odd), we can diagonalize the above Hamiltonian in each subspace with fixed parity. Numerically, we have truncated the infinite matrix by choosing $n_{\max} = 21$, $m_{\max} = 10$ for odd space and $n_{\max} = 20, m_{\max} = 10$ for even space.

B2. Mean photon number

After diagonalizing the matrix (B1), we can obtain the eigenenergy (quasi-energy) ε_j and the corresponding eigenstate

$$|\psi_j(t)\rangle = \sum_{m=-\infty}^{\infty}\sum_{n=0}^{\infty}\left(C^j_{m,n}|e,n\rangle\,\mathrm{e}^{\mathrm{i}m\omega t} + D^j_{m,n}|g,n\rangle\,\mathrm{e}^{\mathrm{i}m\omega t}\right), \tag{B3}$$

where $C^j_{m,n}$ and $D^j_{m,n}$ represent the probabilities of the polariton in the set of basis states $|e,n\rangle\,\mathrm{e}^{\mathrm{i}m\omega t}$ and $|g,n\rangle\,\mathrm{e}^{\mathrm{i}m\omega t}$, respectively.

In the Floquet space, the time-periodic-averaged mean photon number is defined as

$$\begin{aligned}n^j_{\rm ph} &\equiv \frac{1}{T}\int_0^T \mathrm{d}t\langle\psi_j(t)|\hat{a}^\dagger\hat{a}|\psi_j(t)\rangle\\ &= \frac{1}{T}\int_0^T \mathrm{d}t\Big[\sum_{m'}\sum_{n'}\left(C^{j*}_{m',n'}\,\mathrm{e}^{-\mathrm{i}m'\omega t}\langle n',e| + D^{j*}_{m',n'}\,\mathrm{e}^{-\mathrm{i}m'\omega t}\langle n',g|\right)\end{aligned}$$

$$
\begin{aligned}
&\times \hat{a}^{\dagger}\hat{a}\sum_{m}\sum_{n}\left(C^{j}_{m,n}|e,n\rangle\,\mathrm{e}^{\mathrm{i}m\omega t}+D^{j}_{m,n}|g,n\rangle\,\mathrm{e}^{\mathrm{i}m\omega t}\right)\Big]\\
&=\sum_{m'}\sum_{m}\sum_{n'}\sum_{n}\left[\frac{1}{T}\int_{0}^{T}\mathrm{d}t\,\mathrm{e}^{-\mathrm{i}(m'-m)\omega t}C^{j*}_{m',n'}C^{j}_{m,n}\langle n',e|\hat{a}^{\dagger}\hat{a}|e,n\rangle\right.\\
&\quad\left.+\frac{1}{T}\int_{0}^{T}\mathrm{d}t\,\mathrm{e}^{-\mathrm{i}(m'-m)\omega t}D^{j*}_{m',n'}D^{j}_{m,n}\langle n',g|\hat{a}^{\dagger}\hat{a}|g,n\rangle\right]\\
&=\sum_{m'}\sum_{m}\sum_{n'}\sum_{n}\left(C^{j*}_{m',n'}C^{j}_{m,n}n+D^{j*}_{m',n'}D^{j}_{m,n}n\right)\delta_{m',m}\delta_{n',n}\\
&=\sum_{m}\sum_{n}n\left(|C^{j}_{m,n}|^{2}+|D^{j}_{m,n}|^{2}\right),
\end{aligned}
\tag{B4}
$$

where we have used the relations $\frac{1}{T}\int_{0}^{T}\mathrm{e}^{-\mathrm{i}(m'-m)\omega t}\mathrm{d}t=\delta_{m',m}$ and $\langle n',e|\hat{a}^{\dagger}\hat{a}|e,n\rangle=n\delta_{n',n}$.

References

[1] Jaynes E T and Cummings F W 1963 *Proc. IEEE* **51** 89
[2] Shore B W and Knight P L 1993 *J. Mod. Opt.* **40** 1195
[3] Cummings F W 1965 *Phys. Rev.* **140** A1051
[4] Eberly J H, Narozhny N B and Sanchez-Mondragon J J 1980 *Phys. Rev. Lett.* **44** 1323
[5] Narozhny N B, Sanchez-Mondragon J J and Eberly J H 1981 *Phys. Rev. A* **23** 236
[6] Knight P L and Radmore P M 1982 *Phys. Rev. A* **26** 676
[7] Rempe G, Walther H and Klein N 1987 *Phys. Rev. Lett.* **58** 353
[8] Phoenix S J D and Knight P L 1991 *Phys. Rev. A* **44** 6023
[9] Brune M, Haroche S, Raimond J M, Davidovich L and Zagury N 1992 *Phys. Rev. A* **45** 5193
[10] Bužek V, Moya-Cessa H, Knight P L and Phoenix S J D 1992 *Phys. Rev. A* **45** 8190
[11] Brune M, Hagley E, Dreyer J, Maître X, Maali A, Wunderlich C, Raimond J M and Haroche S 1996 *Phys. Rev. Lett.* **77** 4887
[12] Furuya K, Nemes M C and Pellegrino G Q 1998 *Phys. Rev. Lett.* **80** 5524
[13] Sun Q, Hu J, Wen L, Pu H and Ji A C 2018 *Phys. Rev. A* **98** 033801
[14] Wallraff A, Schuster D I, Blais A, Frunzio L, Huang R-S, Majer J, Kumar S, Girvin S M and Schoelkopf R J 2004 *Nature* **431** 162
[15] Hofheinz M, Wang H, Ansmann M, Bialczak R C, Lucero E, Neeley M, O'Connell A D, Sank D, Wenner J, Martinis J M and Cleland A N 2009 *Nature* **459** 546
[16] LaHaye M D, Suh J, Echternach P M, Schwab K C and Roukes M L 2009 *Nature* **459** 960
[17] Niemczyk T, Deppe F, Huebl H, Menzel E P, Hocke F, Schwarz M J, Garcia-Ripoll J J, Zueco D, Hümmer T, Solano E, Marx A and Gross R 2010 *Nat. Phys.* **6** 772
[18] Casanova J, Romero G, Lizuain I, García-Ripoll J J and Solano E 2010 *Phys. Rev. Lett.* **105** 263603
[19] Forn-Díaz P, Lisenfeld J, Marcos D, García-Ripoll J J, Solano E, Harmans C J P M and Mooij J E 2010 *Phys. Rev. Lett.* **105** 237001
[20] Chen Q H, Li L, Liu T and Wang K L 2012 *Chin. Phys. Lett.* **29** 014208
[21] Baust A, Hoffmann E, Haeberlein M, Schwarz M J, Eder P, Goetz J, Wulschner F, Xie E, Zhong L, Quijandría F, Zueco D, García Ripoll J J, García-Álvarez L, Romero G, Solano E, Fedorov K G, Menzel E P, Deppe F, Marx A and Gross R 2016 *Phys. Rev. B* **93** 214501
[22] Forn-Díaz P, Lamata L, Rico E, Kono J and Solano E 2019 *Rev. Mod. Phys.* **91** 025005
[23] Milonni P W, Ackerhalt J R and Galbraith H W 1983 *Phys. Rev. Lett.* **50** 966
[24] Emary C and Brandes T 2003 *Phys. Rev. E* **67** 066203
[25] Chen Q H, Yang Y, Liu T and Wang K L 2010 *Phys. Rev. A* **82** 052306
[26] Liu T, Feng M and Wang K L 2011 *Phys. Rev. A* **84** 062109
[27] Naderi M H 2011 *J. Phys. A: Math. Theor.* **44** 055304
[28] Wang Y M and Du G and Liang J Q 2012 *Chin. Phys. B* **21** 044207
[29] Tang N, Xu T T and Zeng H S 2013 *Chin. Phys. B* **22** 030304
[30] Mirzaee M and Batavani M 2015 *Chin. Phys. B* **24** 040306
[31] Rabi I I 1936 *Phys. Rev.* **49** 324
[32] Rabi I I 1937 *Phys. Rev.* **51** 652
[33] Braak D 2011 *Phys. Rev. Lett.* **107** 100401
[34] Braak D 2019 *Symmetry* **11** 1259
[35] Dong Y H, Zhang W J, Liu J and Xie X T 2019 *Chin. Phys. B* **28** 114202
[36] Feranchuk I D, Komarov L I and Ulyanenkov A P 1996 *J. Phys. A: Math. Gen.* **29** 4035
[37] Tur É A 2000 *Opt. Spectrosc.* **89** 574
[38] Pan F, Guan X, Wang Y and Draayer J P 2010 *J. Phys. B: At. Mol. Opt. Phys.* **43** 175501
[39] Chen Q H, Liu T, Zhang Y Y and Wang K L 2011 *Europhys. Lett.* **96** 14003
[40] He S, Wang C, Chen Q H, Ren X Z, Liu T and Wang K L 2012 *Phys. Rev. A* **86** 033837
[41] Irish E K, Gea-Banacloche J, Martin I and Schwab K C 2005 *Phys. Rev. B* **72** 195410
[42] Irish E K 2007 *Phys. Rev. Lett.* **99** 173601
[43] Zhang Y Y, Chen Q H and Zhao Y 2013 *Phys. Rev. A* **87** 033827
[44] Zhang Y W, Chen G, Yu L X, Liang Q F, Liang J Q and Jia S T 2011 *Phys. Rev. A* **83** 065802
[45] Yu L X, Zhu S Q, Liang Q F, Chen G and Jia S T 2012 *Phys. Rev. A* **86** 015803
[46] Liu M X, Ying Z J, An J H and Luo H G 2015 *New J. Phys.* **17** 043001
[47] Ying Z J, Liu M X, Luo H G, Lin H Q and You J Q 2015 *Phys. Rev. A* **92** 053823
[48] Mao B B, Liu M X, Wu W, Li L S, Ying Z J and Luo H G 2018 *Chin. Phys. B* **27** 054219
[49] Gan C J and Zheng H 2010 *Eur. Phys. J. D* **59** 473
[50] Mirzaee M and Kamani N 2013 *Chin. Phys. B* **22** 094203
[51] Wang Z H and Zhou D L 2013 *Chin. Phys. B* **22** 114205
[52] Wang Y M and Haw J Y 2015 *Phys. Lett. A* **379** 779
[53] Cong L, Sun X M, Liu M X, Ying Z J and Luo H G 2017 *Phys. Rev. A* **95** 063803
[54] Rahav S, Gilary I and Fishman S 2003 *Phys. Rev. A* **68** 013820
[55] Goldman N and Dalibard J 2014 *Phys. Rev. X* **4** 031027
[56] Eckardt A and Anisimovas E 2015 *New J. Phys.* **17** 093039
[57] Bukov M, D'Alessio L and Polkovnikov A 2015 *Adv. Phys.* **64** 139
[58] Eckardt A 2017 *Rev. Mod. Phys.* **89** 011004
[59] Rodriguez-Vega M, Lentz M and Seradjeh B 2018 *New J. Phys.* **20** 093022
[60] Oka T and Aoki H 2009 *Phys. Rev. B* **79** 081406(R)
[61] Hemmerich A 2010 *Phys. Rev. A* **81** 063626
[62] Bermudez A, Schaetz T and Porras D 2012 *New J. Phys.* **14** 053049
[63] Jotzu G, Messer M, Desbuquois R, Lebrat M, Uehlinger T, Greif D and Esslinger T 2014 *Nature* **515** 237
[64] Gulácsi B and Dóra B 2015 *Phys. Rev. Lett.* **115** 160402
[65] Meinert F, Mark M J, Lauber K, Daley A J and Nägerl H C 2016 *Phys. Rev. Lett.* **116** 205301
[66] Mikami T, Kitamura S, Yasuda K, Tsuji N, Oka T and Aoki H 2016 *Phys. Rev. B* **93** 144307
[67] Rodriguez-Vega M and Seradjeh B 2018 *Phys. Rev. Lett.* **121** 036402